Ice Technology Conference, MIT, 1986

Numerical Modelling of Ice-Structure Interaction

F.S. Chehayeb, J.J. Connor and S.S. Sunder
Department of Civil Engineering, Massachusetts Institute of Technology, Cambridge, MA 02129, U.S.A.

INTRODUCTION

The interaction of an ice sheet with a vertically faced (and usually rigid) indenter is an important loading condition for cylindrical structures and for conical structures with grounded rubble pile or accreted ice foot. In general, this indentation phenomenon is characterized by the simultaneous occurrence of viscous (rate-dependent) and fracture behavior.

Several theoretical models based on approximate methods of analysis that idealize the ice sheet as a continuum have been proposed for predicting global ice forces. These include: (1) the upper and lower bound, plasticity type solutions of Michel and Toussaint (1977), Croasdale et al.(1977), and Ralston (1978), (2) the reference stress, power law creep solution of Ponter et al.(1983) , and (3) the upper bound, power law creep solutions of Bruen, (1984) Vivatrat (1985) , and Ting and Shyam Sunder (1985) . The plasticity type models require empirical definition of an average strain rate measure to account for the viscous behavior of ice, the reference stress approach accounts for the effect of variability in material constants in an approximate sense, and the upper bound, power law creep solutions require accurate specification of ice sheet kinematics. No equivalent theoretical models exist for the case where either pure (linear elastic) fracture or combined viscous and fracture effects dominate.

Theoretical predictions of interface pressures are not generally available. However, Ting and Shyam Sunder (1985) have applied the (approximate) strain path method of analysis, originally developed for deep penetration problems in soil mechanics by Baligh (1984), to study interface pressures during plane strain indentation. Their results for a power law creep model of ice showed that normal interface pressures may be 0.5-1 times the global pressure. They also found that interface adfreeze and friction stresses can significantly influence ice pressures.

The "continuum" predictions of ice pressures may in many cases be too high by a factor of 2-10. Four major factors can explain this uncertainty: (i) incomplete modeling of the mechanical behavior of ice, including temperature and fracture effects, (ii) empiricism in the theoretical models resulting from the use of approximate analysis methods, (iii) inadequate modelling of contact forces at the ice-structure interface, and (iv) ignoring the effects of size on material strength.

A study of ice indentation in the creeping mode is important for two reasons: (a) creep is the predominant mode of deformation for artificial islands in the Arctic nearshore region during "breakout" and/or steady indentation conditions occurring in the winter, and (b) stresses, strains, and strainrates within the continuum resulting from creep are necessary to predict the initiation and possibly even the propagation of cracks when viscous effects influence fracture behavior.

This paper is concerned with the development and application of a finite element method of analysis for studying global and local pressures generated on a rigid, vertical surface during sea ice deformations in the creeping mode. Numerical simulations are performed under plane stress conditions to asess the influence of interface adfreeze and friction on predicted pressures. The results are compared with those based on approximate methods of analysis.

FINITE ELEMENT FORMULATION GOVERNING EQUATIONS

For general viscoplastic behavior, which includes creep, it is convenient to work with the time derivative form of the governing equations for a solid. They are written here in matrix form:

$$
\begin{array}{lll}
\text{Equilibrium} & \underline{L}\,\dot{\underline{\sigma}} + \dot{\underline{b}} = \underline{0} & \text{in } \Omega \\
 & \dot{\underline{p}} = \underline{\alpha}\,\dot{\underline{\sigma}} & \text{on } \Gamma \\
\text{Strain-displacement} & \dot{\underline{\epsilon}} = \underline{L}^T\,\dot{\underline{u}} & \text{in } \Omega \\
\text{Strain-stress} & \dot{\underline{\epsilon}} = f\,(\dot{\underline{\sigma}}, \underline{\sigma}, T) & \text{in } \Omega
\end{array}
\qquad (1)
$$

where $\underline{\sigma}$, $\underline{\epsilon}$ are stress and strain vectors; $\underline{u}$ is the displacement vector; $\underline{p}$, $\underline{b}$ are surface and body force intensities; $\underline{L}$ is a rectangular matrix containing partial derivatives with respect to the spatial coordinates; T is the temperature; the dot superscript denotes differentiation with respect to time; Ω denotes the volume and Γ the surface domain.

Weighting the equilibrium equations with a virtual velocity and integrating by parts results in the requirement

$$\int_{\Omega} \dot{\underline{\sigma}}^T \delta\dot{\underline{\epsilon}}\, d\Omega = \int_{\Omega} \dot{\underline{b}}^T \delta\dot{\underline{u}}\, d\Omega + \int_{\Gamma} \dot{\underline{p}}^T \delta\dot{u}\, d\Gamma \tag{2}$$

Equation (2) is the basis for the Finite Element implementation. One expresses $\underline{u}$ in terms of modal values, $\underline{U}$, and interpolation functions, $\underline{\phi}$:

$$\underline{u} = \underline{\phi}\, \underline{U}$$

$$\dot{\underline{u}} = \underline{\phi}\, \dot{\underline{U}} \tag{3}$$

evaluates the strain measures,

$$\dot{\underline{\epsilon}} = \underline{L}^T \underline{\phi}\, \dot{\underline{U}} = \underline{B}\, \dot{\underline{U}} \tag{4}$$

and requires (2) to be satisfied for arbitrary $\delta\dot{\underline{U}}$. The "weighted" equilibrium equations can be interpreted as conditions on the equivalent nodal forces, corresponding to the external actions ($\underline{b}$,$\underline{p}$) and the internal actions ($\underline{\sigma}$):

$$\dot{\underline{P}}_{INT} = \dot{\underline{P}}_{EXT}$$

$$\dot{\underline{P}}_{INT} = \int_{\Omega} \underline{B}^T \dot{\underline{\sigma}}\, d\Omega$$

$$\dot{\underline{P}}_{EXT} = \int_{\Omega} \underline{\phi}^T \dot{\underline{b}}\, d\Omega + \int \underline{\phi}^T \dot{\underline{p}}\, d\Omega \tag{5}$$

The problem reduces to finding $\underline{U}$ such that (5) is satisfied for all time, t.

DETERMINATION OF TIME-HISTORY RESPONSE

Assuming (5) is satisfied at time t_n, we move to the next time point, t_{n+1} using the integrated form of (5):

$$\Delta\underline{P}_{INT} = \Delta\underline{P}_{EXT}$$

$$\Delta\underline{P}_{INT} = \int_{t_n}^{t_{n+1}} \left[\int_{\Omega} \underline{B}^T \dot{\sigma}\, d\Omega \right] dt = \int \underline{B}^T \Delta\underline{\sigma}\, d\Omega$$

$$\Delta \underline{P}_{EXT} = \int_{\Omega} \underline{\phi}^T \Delta \underline{b} d\Omega + \int_{\Gamma} \underline{\phi}^T \Delta \underline{p} d\Gamma \qquad (6)$$

With (6), our task is to find $\Delta \underline{U} = \underline{U}_{n+1} - \underline{U}_n$ such that the corresponding stress increment, $\Delta \underline{\sigma}$, satisfies the incremental equilibrium equation.

MATERIAL MODELLING

In general, the strain rate can be written as the sum of elastic and inelastic terms,

$$\dot{\underline{\epsilon}} = \dot{\underline{\epsilon}}_e + \dot{\underline{\epsilon}}_I \qquad (7)$$

We consider in this discussion the elastic component to be linear,

$$\dot{\underline{\epsilon}}_e = \underline{C}\, \dot{\underline{\sigma}} \qquad (8)$$

and the inelastic component to be due to plasticity and creep,

$$\dot{\underline{\epsilon}}_I = \dot{\underline{\epsilon}}_p + \dot{\underline{\epsilon}}_c \qquad (9)$$

Combining (8) and (9) and integrating $\dot{\underline{\sigma}}$ between t_n and t_{n+1} results in

$$\Delta \underline{\sigma} = \underline{D}(\Delta \underline{\epsilon} - \Delta \underline{\epsilon}_I)$$

$$\underline{D} = \underline{C}^{-1} \qquad (10)$$

Noting (4),

$$\Delta \underline{\epsilon} = \underline{B}\, \Delta \underline{U} \qquad (11)$$

The inelastic contribution,

$$\Delta \underline{\epsilon}_I = \int_{t_n}^{t_{n+1}} (\dot{\underline{\epsilon}}_p + \dot{\underline{\epsilon}}_c) dt \qquad (12)$$

has to be evaluated in an approximate manner since these strain rates are generally nonlinear functions of stress and stress rates. We discuss this aspect in more detail later.

AN ITERATION STRATEGY

Introducing (10), (11) in (6) yields

$$\underline{K}\,\Delta\underline{U} = \Delta\underline{P}_{EXT} + \int_{\Omega} \underline{B}^T\underline{D}\,\Delta\underline{\epsilon}_I\,d\Omega$$

$$\underline{K} = \int_{\Omega} \underline{B}^T\underline{D}\,\underline{B}\,d\Omega \qquad (13)$$

The problem with (13) is the $\Delta\underline{\epsilon}_I$ term; it is a nonlinear function of $\underline{\sigma}$, $\dot{\underline{\sigma}}$ and one has to resort to an iterative scheme. Assuming $\Delta\underline{\epsilon}_I$ is known, we can determine $\Delta\underline{U}$, then $\Delta\underline{\epsilon}$ with (11) and $\Delta\underline{\sigma}$ with (10). With this estimate for $\Delta\underline{\sigma}$, we can generate a new estimate for $\Delta\underline{\epsilon}_I$ and repeat the process. There are two levels of iteration:

<u>Level 1</u> Iteration on $\Delta\underline{U}$

$$\underline{K}\,\Delta\underline{U}^{(i+1)} = \Delta\underline{P}_{EXT} + \int \underline{B}^T\underline{D}\,\Delta\underline{\epsilon}_I^{(i)}\,d\Omega \qquad (14)$$

<u>Level 2</u> For a given $\Delta\underline{U}$, find $\Delta\underline{\epsilon}_I$

$$\Delta\underline{\epsilon}_I^{(i+1)} = \int_{t_n}^{t_{n+1}} \left|\dot{\underline{\epsilon}}_p + \dot{\underline{\epsilon}}_c\right|_{\Delta U^{(i+1)}} dt \qquad (15)$$

The latter step, i.e., evaluating (15) presents a major difficulty when the inelastic strain is significantly greater than the elastic strain. This is usually the case for ice. In what follows, we discuss how (15) is evaluated.

EVALUATION OF THE INCREMENTAL INELASTIC STRAIN

To establish the basic approach, we consider first the case where the material is linearly viscous and write

$$\dot{\underline{\epsilon}}_p = \underline{C}_p\,\dot{\underline{\sigma}}$$

$$\dot{\underline{\epsilon}}_c = \underline{C}_c\,\underline{\sigma} \qquad (16)$$

where $\underline{C}_p$, $\underline{C}_c$ are considered to be constant. Integrating (16) results in

$$\Delta\underline{\epsilon}_I = \underline{C}_P\, \Delta\underline{\sigma} + \underline{C}_c \int_{t_n}^{t_{n+1}} \underline{\sigma}\, dt \tag{17}$$

To proceed further, we need to approximate the integral. A convenient choice is the generalized Crank-Nicholson rule,

$$\int_{t_n}^{t_{n+1}} f(t)dt = \Delta t \left[(1-\alpha)f_n + \alpha f_{n+1}\right] \tag{18}$$

where α is a parameter. Applying (18) to (17) and rearranging leads to:

$$(\underline{C}_p + \alpha\Delta t\underline{C}_c)\underline{\sigma}_{n+1} = \Delta\underline{\epsilon}_I + (\underline{C}_p - (1-\alpha)\Delta t\underline{C}_c)\underline{\sigma}_n \tag{19}$$

Our objective is to determine $\Delta\underline{\epsilon}_I$. However, (19) shows that we must also find $\underline{\sigma}_{n+1}$. The solution is to combine (19) with (10), (11) expressed as

$$\begin{aligned} \Delta\underline{\epsilon}_I &= \Delta\underline{\epsilon} - C\Delta\underline{\sigma} \\ &= \underline{B}\Delta\underline{U} - \underline{C}\Delta\underline{\sigma} \end{aligned} \tag{20}$$

The final result is

$$\begin{aligned} (\underline{C} + \underline{C}_p + \alpha\Delta t\underline{C}_c)\underline{\sigma}_{n+1} &= \underline{B}\Delta\underline{U} + (\underline{C} + \underline{C}_p - (1-\alpha)\Delta t\underline{C}_c)\underline{\sigma}_n \\ \Delta\underline{\epsilon}_I &= \underline{B}\, \Delta\underline{U} - \underline{C}\, (\underline{\sigma}_{n+1} - \underline{\sigma}_n) \end{aligned} \tag{21}$$

Given $\Delta\underline{U}^{(i+1)}$, we find $\underline{\sigma}_{n+1}^{(i+1)}$, then $\Delta\underline{\epsilon}_I^{(i+1)}$, and using $\Delta\underline{\epsilon}_I^{(i+1)}$, evaluate $\Delta\underline{U}^{(i+2)}$ with (14). A stability analysis of the first order scalar differential equation,

$$\dot{y} + \lambda y = f(t) \tag{22}$$

shows that the numerical integration is unconditionally stable only for $\alpha \geq 0.5$. A value of α equal to 1 corresponds to applying a first order backward difference operator to (16) at time t_{n+1} while $\alpha = 0.5$ is the classical trapezoidal rule.

The approach outlined above can be extended to nonlinear material behavior by considering $\underline{C}_p$, $\underline{C}_c$ in (16) to be functions of $\underline{\sigma}$, $\dot{\underline{\sigma}}$. In this case, they cannot be moved outside the time integral, and (19) expands to

$$\alpha\, \Delta t\, (\underline{C}_{p,n+1}\, \dot{\underline{\sigma}}_{n+1} + \underline{C}_{c,n+1}\, \underline{\sigma}_{n+1}) = \Delta \underline{\epsilon}_I - (1-\alpha)\Delta t\, (\underline{C}_{p,n}\, \dot{\underline{\sigma}}_n + \underline{C}_{c,n}\, \underline{\sigma}_n) \tag{23}$$

We combine (23) with (20) and replace $\dot{\underline{\sigma}}_{n+1}$ with a first order backward difference. The final form is

$$\begin{aligned}(\underline{C} + \alpha\underline{C}_{p,n+1} + \alpha\Delta t\, \underline{C}_{c,n+1})\underline{\sigma}_{n+1} = {} & \underline{B}\, \Delta\underline{U} \\ & + (\underline{C} + \alpha\underline{C}_{p,n+1} - (1-\alpha)\, \Delta t\, \underline{C}_{c,n})\, \underline{\sigma}_n \\ & - (1-\alpha)\, \Delta t\, \underline{C}_{p,n}\, \dot{\underline{\sigma}}_n\end{aligned}$$

where

$$\dot{\underline{\sigma}}_{n+1} = \frac{1}{\Delta t}(\underline{\sigma}_{n+1} - \underline{\sigma}_n) \tag{24}$$

We need to iterate on (24) since $\underline{C}_{p,n+1}$ and $\underline{C}_{c,n+1}$ depend on $\underline{\sigma}_{n+1}$. The simplest approach is to treat the coefficient of $\underline{\sigma}_{n+1}$ in (24) as known and solves by successive substitutions the modified set of equations:

$$\begin{aligned}\underline{E}^{(k)}\, \underline{\sigma}_{n+1}^{(k+1)} &= \underline{F}_n \\ \underline{E}^{(k)} &= \underline{C} + \Big[\alpha\, \underline{C}_{p,n+1} + \alpha\Delta t\underline{C}_{c,n+1}\Big]_{\underline{\sigma}_{n+1}^{(k)}}\end{aligned} \tag{25}$$

This strategy is efficient when creep deformation is not dominant. Experience has shown that $\alpha=1$ yields the "best" results when Δt is large. For small Δt, $\alpha=0.5$ is more accurate.

Convergence degenerates as the creep strain becomes more important in comparison to the elastic strain, and an alternate iterative scheme is necessary. The "next" level scheme is generated by expanding the left hand side of (25) in a Taylor series about $\underline{\sigma}_{n+1}^{(k)}$ and corresponds to the Newton-Raphson method. The equations for this scheme have the general form:

$$\frac{\partial}{\partial\underline{\sigma}_{n+1}}(\underline{E}\, \underline{\sigma}_{n+1})_{\underline{\sigma}_{n+1}^{(k)}}\, (\underline{\sigma}_{n+1}^{(k+1)} - \underline{\sigma}_{n+1}^{(k)}) = \underline{F}_n - (\underline{E}\, \underline{\sigma}_{n+1})_{\underline{\sigma}_{n+1}^{(k)}} \tag{26}$$

In order to evaluate the derivative of $\underline{E}$, the form of $\underline{C}_p$ and $\underline{C}_c$ are required. This is treated in the following section. Iteration is necessary at each integration point of an element. Convergence is considered to be achieved when the maximum absolute value of the relative change in integration point stresses is less than 10^{-3}. With the successive substitution scheme, 10-12, iterations are typically required for a creep dominant behavior. This effort is reduced to about four iterations with the Newton-Raphson approach. Allowing for the increased effort per cycle, the net reduction is approximately 50%.

CONSTITUTIVE RELATIONS FOR THE CREEP MODE

We present in this section the strain rate relations for creep based on a uni-axial power law model and orthotropic material behavior. Our starting point is the scalar uniaxial relation for creep strain-rate,

$$\epsilon_c = b\sigma^N = \frac{\partial\phi}{\partial\sigma}$$

$$\phi = \frac{b}{N+1}\,\sigma^{N+1} \tag{27}$$

The extension to the multi-dimensional stress state is accomplished by introducing an effective stress measure, σ_E, taking ϕ to be a function of σ_E, and requiring

$$d\phi = \frac{\partial\phi}{\partial\sigma_E}\,d\sigma_E \equiv \dot{\underline{\epsilon}}_c^{\,T}\,d\underline{\sigma} \tag{28}$$

We express σ_E as

$$\sigma_E = f(\underline{\sigma}) \tag{29}$$

Then,

$$d\sigma_E = \frac{\partial f}{\partial\underline{\sigma}}\,d\underline{\sigma} \tag{30}$$

and it follows from (28) that

$$\dot{\underline{\epsilon}}_c = \frac{d\phi}{d\sigma_E}\left(\frac{\partial f}{\partial\underline{\sigma}}\right)^T \tag{31}$$

We had expressed (31) as (see (16)):

$$\dot{\underline{\epsilon}}_c = \underline{C}_c \, \underline{\sigma} \tag{32}$$

One determines $\underline{C}_c$ by expanding ${}^{\partial f}/_{\partial \underline{\sigma}}$ and ${}^{d\phi}/_{d\sigma_E}$.

We suppose the material is orthotropic and each direction follows the power law for creep. The "orthotropic" form for f is

$$\sigma_E = f(\underline{\sigma}) = \left[\underline{\sigma}^T \underline{A} \, \underline{\sigma}\right]^{1/2}$$

$$\underline{\sigma} = [\sigma_1, \sigma_2, \sigma_3, \tau_{12}, \tau_{23}, \tau_{31}]$$

$$A = \begin{bmatrix} 1+a_3 & -1 & -a_3 & 0 & 0 & 0 \\ -1 & 1+a_2 & -a_2 & 0 & 0 & 0 \\ -a_3 & -a_2 & a_2+a_3 & 0 & 0 & 0 \\ 0 & 0 & 0 & a_4 & 0 & 0 \\ 0 & 0 & 0 & 0 & a_5 & 0 \\ 0 & 0 & 0 & 0 & 0 & a_6 \end{bmatrix} \tag{33}$$

Then,

$$\frac{\partial f}{\partial \underline{\sigma}} = \frac{1}{2f} \frac{\partial}{\partial \underline{\sigma}} (\underline{\sigma}^T \, \underline{A} \, \underline{\sigma}) = \frac{1}{f}(\underline{A} \, \underline{\sigma})^T \tag{34}$$

Taking

$$\phi = \frac{b_E}{N+1} \sigma_E^{N+1} \tag{35}$$

results in

$$\underline{C}_c = b_E \sigma_E^{N-1} \underline{A} \tag{36}$$

This form satisfies the incompressibility condition, $\dot{\epsilon}_V = 0$.

The parameters a_2, a_3, and b_E are established by applying three normal loadings,

$$(\sigma_1,0,0,0,0,0) \qquad (0,\sigma_2,0,0,0,0) \qquad (0,0,\sigma_3,0,0,0)$$

and equating the "observed" parameters to the corresponding terms in (36). For $(\sigma_1,0,0,0,0,0)$ we have

$$\sigma_E = (1+a_3)^{1/2}\,\sigma_1$$

$$\dot{\epsilon}_1 = b_1\sigma_1^{\,N} = b_E\left[(1+a_3)^{1/2}\sigma_1\right]^{N-1}\ (1+a_3)\sigma_1 \tag{37}$$

Repeating this operation for the "2" and "3" directions results in three equations for a_2, a_3, b_E.

$$b_1 = (1+a_3)^{\frac{N+1}{2}}\, b_E$$

$$b_2 = (1+a_2)^{\frac{N+1}{2}}\, b_E$$

$$b_3 = (a_2+a_3)^{\frac{N+1}{2}}\, b_E \tag{38}$$

Solving (38) gives

$$a_2\left[-1 + \left[\frac{b_2}{b_3}\right]^{\beta} + \left[\frac{b_1}{b_3}\right]^{\beta}\right] = 1 + \left[\frac{b_2}{b_3}\right]^{\beta} - \left[\frac{b_1}{b_3}\right]^{\beta}$$

$$a_3 = (1+a_2)\left[\frac{b_1}{b_2}\right]^{\beta} - 1$$

$$b_E = b_2\ (1+a_2)^{-1/\beta}$$

$$\beta = 2/(N+1) \tag{39}$$

The parameters a_4, a_5, and a_6 are established by applying three shear loadings,

$(0,0,0,\tau,0,0)$ $(0,0,0,0,\tau,0)$ $(0,0,0,0,0,\tau)$

and procceding in a fashion similar to the one above. This would yield

$$\dot{\epsilon}_4 = b_4\tau^N = b_E\left[\ a_4^{\,1/2}\ \tau\ \right]^{N-1} a_4\ \tau \tag{40}$$

Repeating the operation for "5" and "6", and solving for a_4, a_5, and a_6 yields

$$a_4 = \left[\frac{b_4}{b_E}\right]^{\beta}$$

$$a_5 = \left[\frac{b_5}{b_E}\right]^{\beta}$$

$$a_6 = \left[\frac{b_6}{b_E}\right]^{\beta} \tag{41}$$

When the material is isotropic,

$$b_1 = b_2 = b_3 = b$$

$$b_4 = b_5 = b_6 = G \tag{42}$$

and (39), (41) reduce to

$$a_2 = a_3 = 1$$

$$b_E = b\ (2)^{\frac{N+1}{2}}$$

$$a_4 = a_5 = a_6 = \left[\frac{G}{b\ (2)^{\frac{N+1}{2}}}\right] \tag{43}$$

Using $\underline{C}_C$ defined by (36) we return to the iteration algorithm for the Newton-Raphson method (26), and perform the differentiation with respect to $\underline{\sigma}$. The final result is

$$\frac{\partial}{\partial \underline{\sigma}} (\underline{E}\ \underline{\sigma}) = \underline{C} + (\alpha \Delta t\ b_E\ \sigma_E^{\ N-1}) \left[\underline{A} + \frac{N-1}{\sigma_E^{\ 2}} (\underline{A}\ \underline{\sigma})\ (\underline{A}\ \underline{\sigma})^T\right] \tag{44}$$

COMPUTER IMPLEMENTATION

The current implementation is a two-dimensional version for plane stress problems, while the development of a plane strain version is underway. A four-noded quadrilateral element is currently available. Although an eight-noded quadratic element is often preferred (and will be included in the future), accurate results can and have been obtained with the four-noded element using a finer finite element mesh. The program has the ability to simulate a free or frictional contact between two deformable bodies, i.e., no contact stresses due to adfreeze bond, by defining the interface as a "slideline".

The accuracy of the computer code has been verified in two ways; through the solution of simple test problems, and by comparing the variability in predicted global pressures due to identer diameter, material model parameters, and ice sheet velocity with that predicted by approximate methods of analysis. In both cases, the numerical solutions are accurate to wtihin specified tolerances typically achievable in finite element analyses.

One of the test problems considred a two-dimensional rectangular element subjected to a uniform compressive stress ($\sigma_z = -\sigma$) normal to one of its sides and with normal movement constrained on the other three sides (Fig. 1). A simple analysis shows that for the isotropic power law material model, the lateral stress (σ_y) is given by:

$$\sigma_y = -\sigma_z/2 \left[(1-2\nu)e^{-E\lambda t} - 1 \right]$$

$$\lambda = b\sigma_E^{N-1} \qquad (45)$$

where ν is the Poisson's ratio and E is the Young's modulus. This solution is valid for a constant value of λ, which in an average sense may be defined as its value at steady state. Under steady state conditions, i.e. large t, Eq. (45) shows that the lateral stress is compressive and equal to half the z-stress. Furthermore, the z-strainrate is the creep strainrate and equals $-\lambda\sigma/2$ while the lateral strainrate is zero as it should be for the given boundary conditions. A model consisting of two finite elements verified this analysis.

The choice of time increment is made to satisfy the conflicting requirements of accuracy and computational effort. Experience with the simulations has shown that it is appropriate to consider a time increment which makes the exponent in Eq. (45) equal to 3 in 20 time steps. For values of λ and E typical of ice, the time increment is approximately 100 s.

A series of numerical simulations for a plane ice sheet moving past a rigid circular identer were also carried out. Results are presented in Chehayeb, F. et. al. (1985).

CONCLUSIONS

This study outl
numerical time-
due to creep.
suitable for ar
providing accura

ACKNOWLEDGEMENT

This research
through MIT's
Engineering, a
Interior, Mine
Jaideep Ganguly

REFERENCES

Baligh, M. The
Civil Engineer

Bruen, F. and
Strain-Rate F
Mechanics and

Chehayeb, F.
Mode. OTC Pap

Croasdale, K
Tests to Inve
Glaciology, 1

Glen, J.W. (
of the Royal

Hughes, T.
Nonlinear F
Mechanics an

Michel, S.
Indentation
285-300.

Palmer, A.
Problems. G

Ponter, A.
Sheet on a
Regions Sci

Ralston, T
Ice Sympos

CONCLUSIONS

This study outlines the computational strategy for generating numerical time-history simulation of ice-structure interaction due to creep. Studies show that the approach is economical, suitable for an arbitrary structural geometry, and capable of providing accurate predictions of long term response.

ACKNOWLEDGEMENTS

This research is funded by the Standard Oil Company (Ohio) through MIT's Center for Scientific Excellence in Offshore Engineering, and cosponsored by the U.S. Department of the Interior, Minerals Management Service. The authors thank Jaideep Ganguly and Seng Ting for their assistance.

REFERENCES

Baligh, M. The Strain Path Method (1984) Rpt. R84-01, 761 Civil Engineering Dept., MIT Cambridge 47p.

Bruen, F. and Vivatrat, V. (1984) Ice Force Prediction Based on Strain-Rate Field. Third International Symposium on Offshore Mechanics and Arctic Engineering, New Orleans, 7 p.

Chehayeb, F. et al (1985) Sea Ice Indentation in the Creeping Mode. OTC Paper 5056.

Croasdale, K Morgenstern, M. and Nuttall, J. (1977) Indentation Tests to Investigate Ice Pressures on Vertical Piers. Journal of Glaciology, 19, 81: 310-312.

Glen, J.W. (1955) The Creep of Polycrystalline Ice (1955). Proc. of the Royal Society of London Ser. A, 228, 1175: 519-538.

Hughes, T. (1977). Unconditionally Stable Algorithm for Nonlinear Heat Conduction, Computer Methods for Applied Mechanics and Engineering, 10: 135-139.

Michel, S. and Toussaint, N.(1977) Mechanisms and Theory of Indentation of Ice Plates. Journal of Glaciology, 19, 81: 285-300.

Palmer, A.C. (1967) Creep-Velocity Bounds and Glacier-Flow Problems. Glaciology, 6,46: 479-488.

Ponter, A. et. al., (1983) The Force Exerted by a Moving Ice Sheet on an Offshore Structure Part 1 The Creep Mode. Cold Regions Science and Technology, 8: 109-118.

Ralston, T. (1978) An Analysis of Ice Sheet Indentation, IAHR Ice Symposium, Sweden: 13-31.

Shyam Sunder, S. and Ting, S-K (1985), Ductile to Brittle Transition in Sea Ice under Uniaxial Loading, Prof. of 8th International Conf. on Port and Ocean Engineering under Arctic Conditions, Greenland, 12p.

Snyder, M., Bathe, K. (1981) A Solution Procedure for Thermo-Elastic-Plastic and Creep Problems. Nuclear Engineering and Design, 64: 49-80.

Ting, S-K and Shyam Sunder, S. (1985) Sea Ice Indentation Accounting for Strain-Rate Variation, Proc. of the ASCE Specialty Conference: Arctic '85 - C.E. in the Arctic Offshore, San Francisco, 11p.

Vivatrat, V. and Chen V. (1985) Ice Load Prediction with the Use of a Rate-Dependent Anisotropic Constitutive Law. Prof. of ASCE Specialty Conference: Arctic '85 - C.E.in the Arctic Offshore, San Francisco, 11p.

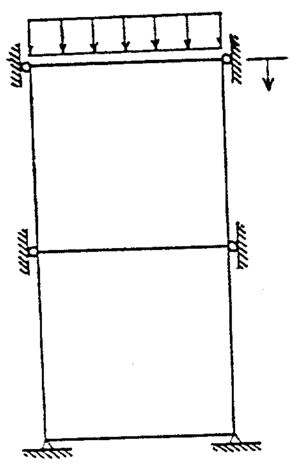

Fig. 1 - Test Problem